Antarct. Meteorite Res., **13**, 78–92, 2000

Natural remanent magnetization of Rumanová chondrite (H5) acquired by the shock metamorphisms S3

M. Funaki[1], I. Túnyi[2], O. Orlický[2] and V. Porubčan[3]

[1]*National Institute of Polar Research, Kaga 1-chome, Itabashi-ku, Tokyo 173–8515*
[2]*Geophysical Institute of Slovak Academy of Sciences, Dúbravská cesta 9, 842 28 Bratislava, Slovakia*
[3]*Astronomical Institute of Slovak Academy of Sciences, Dúbravská cesta 9, 842 28 Bratislava, Slovakia*

Abstract: The natural remanent magnetization (NRM) of Rumanová (H5) chondrite was studied to focus on the shock remagnetization characterized by shock level S3. The NRM was examined by AF and thermal demagnetization, temperature dependencies of magnetization and coercivity, magnetic anisotropy, microscopic features using magnetic fluid technique and chemical compositions. Based on these results, Rumanová carries the stable NRM by a fine-grained taenite with 48 wt%Ni in cloudy taenite, although large amount of the soft NRM component with the magnetic anisotropy is overprinted. These taenite grains were produced by disorder from tetrataenite due to heating between 525°C and 950°C during shock metamorphism when the parent body collided with the asteroids. Rumanová was remagnetized below 530°C in the cooling stage by the local magnetic field from strongly magnetized FeNi grains. From these viewpoints, the NRM of Rumanová was not original, but it was remagnetized during shock metamorphism.

1. Introduction

According to Rojkovič *et al.* (1995, 1997), the Rumanová stony meteorite (4.3 kg) was found in a grain field located 1.25 km NNW from Rumanová Village, western Slovak Republic, in 1994. It was classified as an H5 chondrite showing evidence of recrystallized features in the chondrules and matrix. The recrystallization is ascribed to a weak shock metamorphism of stage S3 which is characterized by parallel planar fractures in olivine based on the classification by Stöffler *et al.* (1991). No opaque veins produced by shock heating have been found. The size of metallic grains of kamacite and taenite varied from 0.1 to 0.6 mm, rarely up to 1 mm. Kamacite with 6.15 to 6.94 at%Ni showed Neumann bands and goethite (α-FeOOH) and limonite were produced from kamacite by weathering alteration. Taenite exhibits normal zoning profiles of Ni from edge to interior from 52.2 to 17.12 at%Ni. Moderate weathering of metal as W2 proposed by Wlotzka (1993) was reported.

We have investigated the basic magnetic properties of Rumanová to determine why this chondrite has a stable NRM. It experienced shock metamorphism of level

S3. Although a part of this study has been published (Funaki *et al.*, 1999), we have investigated this further with new samples and additional data in this study.

2. Natural remanent magnetization

Two block samples A and B without mutual orientation were obtained from Rumanová. They were cut into 5 cubic samples (0.78–1.62 g) respectively with the orientations in the blocks. The samples were numbered as A1–A5 and B1–B5. Several irregular samples without orientation were chipped from A and B blocks. The samples of A1 and A2 and B1–B5 were demagnetized by alternating magnetic field (AF demagnetization) up to 50 mT in steps of 5 mT. Typical AF demagnetization curves of NRM for A1, A2 and B1 are shown in Fig. 1. The intensities (A1: $R=2.511\times10^{-2}$, A2: $R=5.995\times10^{-2}$, B1: $R=4.323\times10^{-2}$ Am^2/kg) were demagnetized steeply up to 20 mT, and then decreased gradually between 25 and 50 mT. The directions of the samples shifted from 0 to 25 mT, although they were more

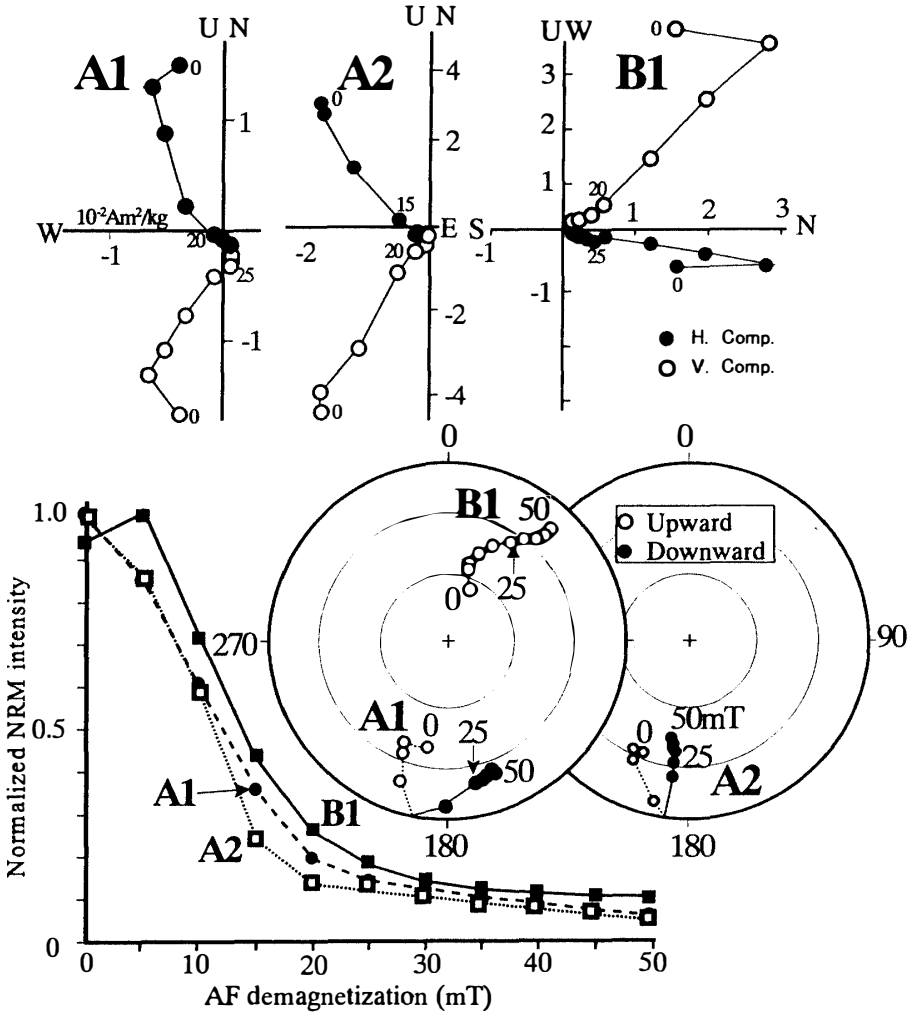

Fig. 1. AF demagnetization curves of NRM of the samples A1, A2 and B1. Upper: Zijderveld projection, lower left: intensity variations, lower right: directional change.

stabile between 25 and 50 mT. These demagnetization behaviors are more easily understood by the description of vector component analyses (Zjiderveld projection); the soft NRM components appeared from 0 to 25 mT and the hard component is recognized by a straight line toward the coordinate axes from 25 to 50 mT. Similar demagnetization curves to samples A1 and A2 were obtained from the other samples in the groups A and B. The optimum AF demagnetization field was, therefore, determined to 30 mT.

The NRM intensities of A1–A5 showed a range of $R=2.021$ to 5.995×10^{-2} Am^2/kg, and the directions (inclination: I, declination: D) made a good cluster, as shown in Fig. 2a. The mean NRM direction is represented as $I=19.9$, $D=186.9$, precision (K) $=52$ and confidence of 95% probability (α_{95}) $=10.7$. When the NRM of samples A1 and A2 were demagnetized to 30 mT, the directions were similar. Although the other 3 samples were not demagnetized at that field, their directions seem to make a cluster. The original samples of B1–B5 having intensity from $R=$ 0.432 to 4.323×10^{-2} Am^2/kg, however, showed scattered NRM directions as shown in Fig. 2b. The directions did not make a cluster when the samples were demagnetized by the optimum field at 30 mT.

Three small irregular samples (B1t, B2t and B3t) without orientations obtained from the sample B1, B2 and B3 were encapsuled into silica tubes under a vacuum of 10^{-3} Pa. They were thermally demagnetized from 30 to 630°C in intervals of 50°C. The demagnetization curves of samples B1t and B2t are shown in Fig. 3. The original NRM intensities of samples ($R=5.968\times10^{-2}$ Am^2/kg for B1t, 6.616×10^{-3} Am^2/kg for B2t) decreased gradually up to 580°C. Their directions were relatively stable to 530°C, while they shifted greatly between 530 and 630°C. In the Zjiderveld

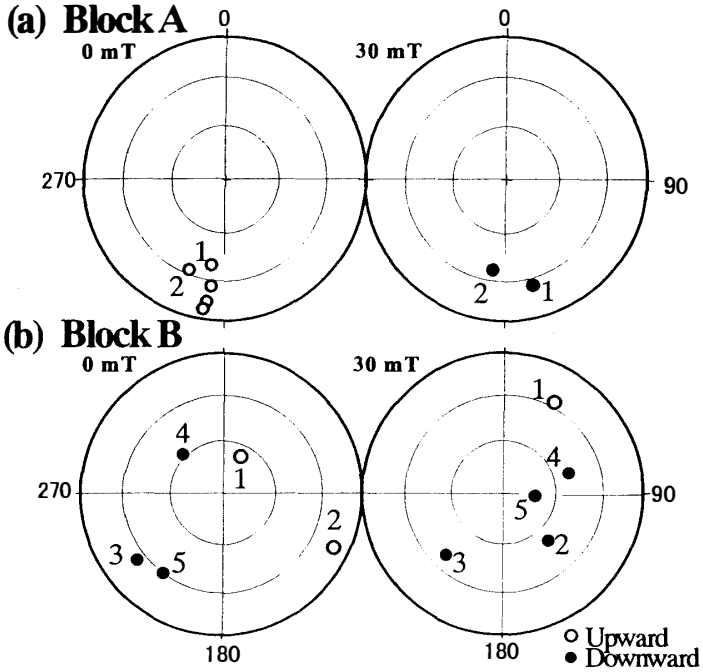

Fig. 2. Distribution of the NRM directions of the samples A1–A5 and B1–B5. Equal area projection.

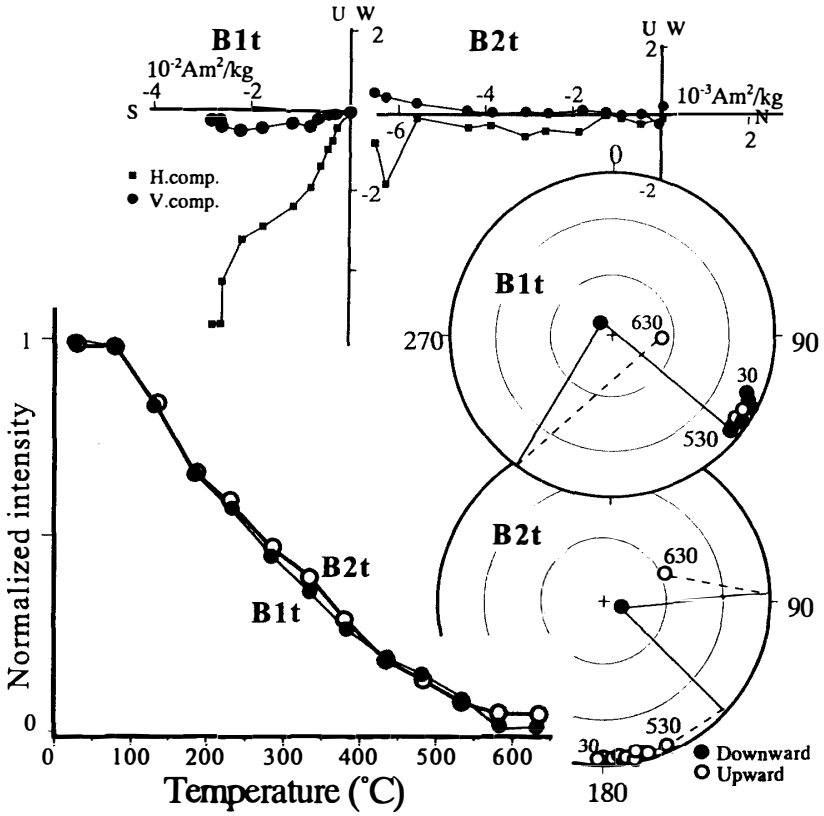

Fig. 3. Thermal demagnetization curves of NRM for the samples B1t and B2t. Upper: Zijderveld projection, lower left: intensity variations, lower right: directional change. Equal area projection.

projection, a hard NRM component was observed between 330 and 530°C for the sample B1t and between 130 and 530°C for the sample B2t, although small zigzag variations appeared on the curve of sample B2t. In the case of sample B3t ($R = 1.235 \times 10^{-2}$ Am^2/kg), the demagnetization curves are essentially consistent with the former samples, but with more zigzag variations. From the thermal demagnetization curves of NRM, the highest NRM blocking temperature at 530°C is obtained from Rumanová.

3. IRM acquisition and susceptibility anisotropy

Sample B1, after AF demagnetization to 50 mT, was given stepwise acquired to the isothermal remanent magnetization (IRM) up to 0.8 T in intervals of 0.05 or 0.1 T toward the direction of the z-axis (downward) at room temperature by pulsed (3 m/s) monopole magnetic field, and then it was demagnetized up to 50 mT in the steps of 5 mT, as shown in Fig. 4. The acquired IRM intensity increased to 0.05 T. It gradually increases between 0.05 and 0.8 T with some small zigzag variations. It seems to be almost saturated (SIRM) at 0.1 T, indicating SIRM$=7.921 \times 10^{-1}$ Am^2/kg at that field. The IRM direction at 0.05 T shifted widely from the original direction, but it was almost stable between 0.05 and 0.8 T. The SIRM direction,

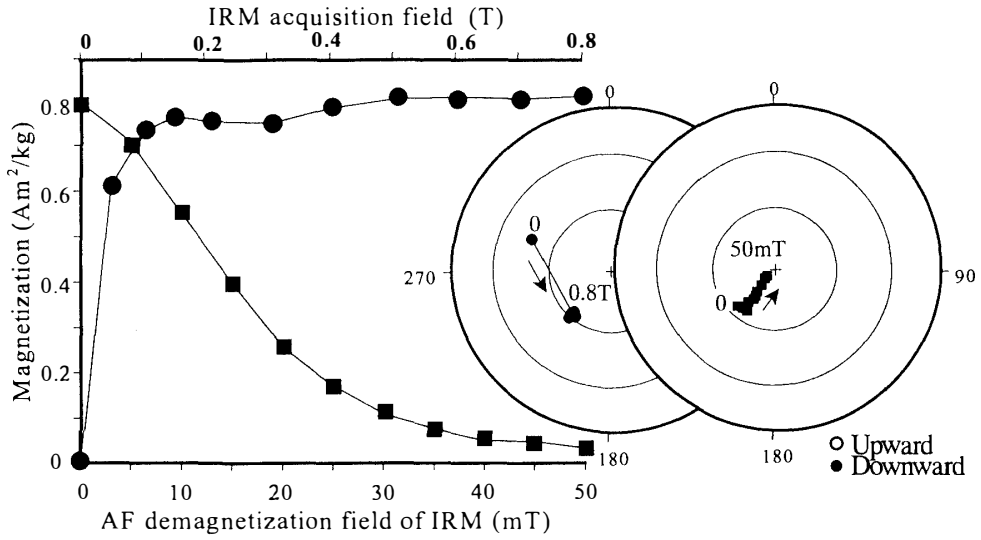

Fig. 4. An IRM acquisition curve up to 0.8 T and its AF demagnetization curve.

however, was not parallel to the applied field direction, deviating 30° from the z-axis.

In the AF demagnetization curve of SIRM, the intensity decreased quickly (soft component) up to 25 mT and gradually decreased (hard component) between 25 and 50 mT, and the residual magnetization at 50 mT is 0.02 Am^2/kg. The direction of SIRM shifted gradually toward the z-axis by progressive AF demagnetization. It suggests that the magnetic grains having high coercivity can acquire IRM in the applied magnetic field direction, but the large grains with low coercivity cannot acquire the IRM in that direction due to the large magnetic anisotropy.

The anisotropy of initial magnetic susceptibility (AMS) of the samples B1–B5 was measured using an oscillating field of 300 A/m of 870 Hz. It was represented by an ellipsoid which is denoted by the values of maximum (K_{max}), intermediate (K_{mid}) and minimum (K_{min}). The range of AMS intensities was $0.62-1.46\times10^{-2}$ (SI), although the average ratio of AMS axes was obtained as $K_{max}=1.17264$, $K_{mid}=0.93331$ and $K_{min}=0.89405$. The individual directions of these axes were scattered widely in the hemisphere. Namely, each sample has large magnetic anisotropy, but the direction of anisotropy axes are random among the samples B1–B5.

4. Thermomagnetic curve and hysteresis properties

The thermomagnetic curves (I_s-T curve) of a small chipped sample B1a (0.2 g in weight) were measured in an external magnetic field of 1.0 T under 10^{-3} Pa atmospheric pressure (Fig. 5). In the 1st run cycle, the curve yielded the clearly defined Curie point (T_c) of taenite at $T_c=550$°C and the phase transition temperatures (T_p) from kamacite (α-phase) to taenite (γ-phase) at $T_p=700$°C in the heating curve and from γ-phase to α-phase at $T_p=580$°C in the cooling curve. A magnetic hump was observed between 80 and 150°C in the 1st-run heating curve. In the

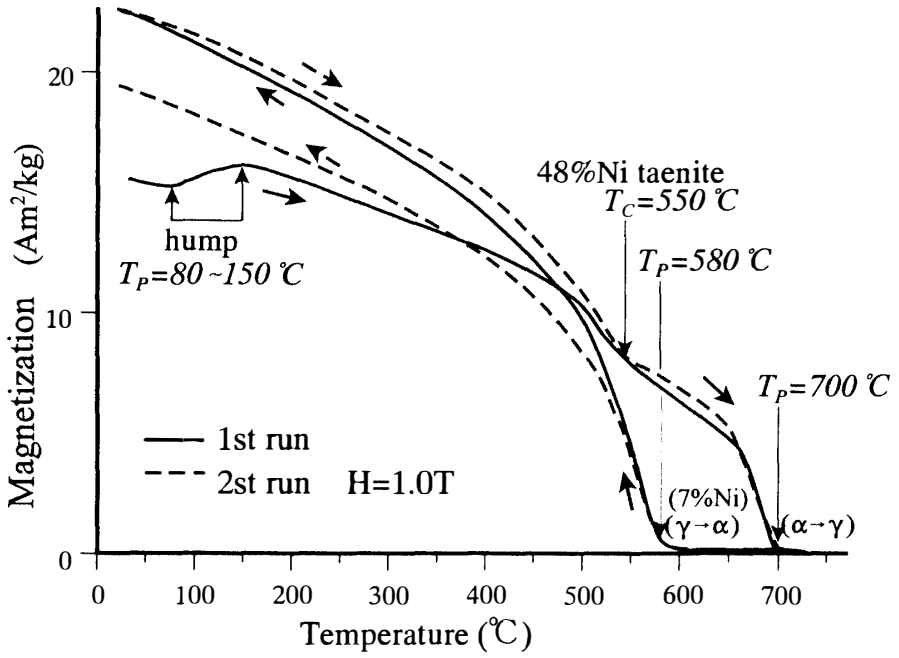

Fig. 5. Thermomagnetic curves of the 1st and 2nd run cycles. External magnetic field of 1.0 T and vacuum of 10^{-3} Pa.

Table 1. Magnetic hysteresis properties at room temperature of sample "a" of Rumanová.

Sample	W (g)	I_S (Am²/kg)	I_R (Am²/kg)	H_C (mT)	H_{RC} (mT)
Original	0.02860	13.85	0.874	10.18	21.31
After heating		17.73	1.993	16.04	33.52

2nd-run curve, the T_c and T_p of iron-nickel (FeNi) were consistent with those of the 1st-run cycle.

The hysteresis loops of sample B1b (0.067 g) was obtained during continuous heating from room temperature to 780°C under the same condition as the I_S-T curve. From the loops, the values of the saturation magnetization (I_S), saturation remanent magnetization (I_R), coercive force (H_C) and remanent coercive force (H_{RC}) were obtained. These values before and after heating are listed in Table 1. As the I_S values increase in proportion to the abundance of FeNi in the sample, the increased value from I_S=13.85 Am²/kg (original) to I_S=17.73 Am²/kg (after heating) suggests formation of ferro- or ferrimagnetic minerals during the heat treatment to 850°C. The H_C=10.18 and H_{RC}=21.31 mT of the original sample increased slightly to H_C=16.04 and H_{RC}=33.52 mT by heating.

The temperature dependence of the H_C values (H_C-T curve) is shown in Fig. 6. The original H_C value gradually decreased to 530°C, and then only insignificant small H_C values appeared up to 750°C in the heating curve. The H_C values increased gradually from 530°C to room temperature in the cooling curve. Almost the same curves are obtained for the H_{RC}-T and I_R-T curves. Namely, the coercivity of Rumanová is lost at 530°C (coercivity Curie point, TH_C), nevertheless I_S value was observed to 700°C in the I_S-T heating curves.

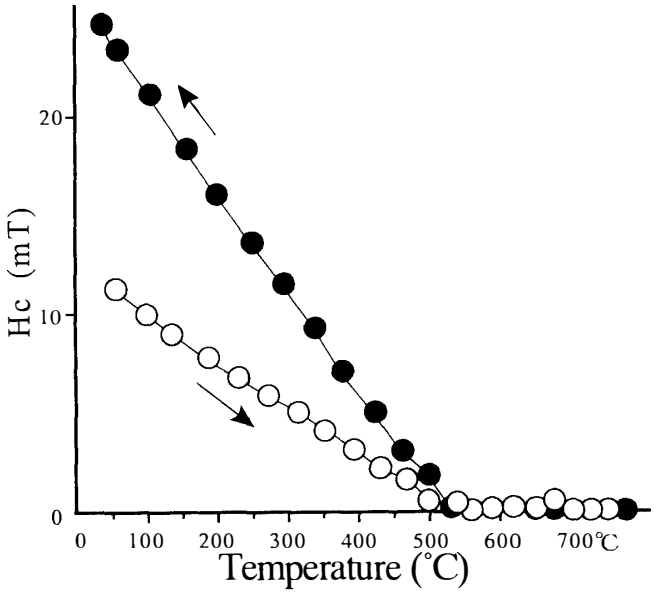

Fig. 6. Temperature dependence of coercivity (H_C) obtained by hysteresis loops.

5. Microscopical observation and chemical composition of FeNi grains

A polished section using diamond paste of 0.5 μm in diameter was etched by NO_2 in order to observe the FeNi grains by reflected light microscopy. The results indicated that the metallic grains consisted of kamacite (K) and taenite (T) associated with plessite (($\alpha+\gamma$)-phase) and cloudy taenite (CT: mixture of fine-grained γ-phase and tetrataenite (γ'-phase)). Topography of one of the representative larger FeNi grains after etching by NO_2 is shown in Fig. 7. In this grain, Neumann bands characterized by straight or bending spindle lines of less than 8 μm width decorated on the kamacite. In the left side of this grain, cloudy taenite with taenite on the edges was observed. Scattered single crystalline troilite grains less than 50 μm in diameter were dominant in the matrix, while twinning of troilite (FeS) grains less than 200 μm were unevenly distributed in contact with larger FeNi grains in the samples. No polycrystalline troilite grains were, however, recognized under the reflected polarized light microscope.

The chemical compositions of Fe, Ni, Co, S and P along the lines A-A′ and B-B′ denoted on Fig. 7 were measured by an electron probe microanalyzer (EPMA) using probe diameter 1 μm (15.0 kV of accelerated voltage) with interval 1.0 μm. These lines pass through K-T-CT-T-K and K-T-K respectively. Their Ni profiles indicated the obscure M-shape profiles in taenite and cloudy taenite, but Fe profiles showed the reversed patterns, as shown in Fig. 7; Ni in taenite and cloudy taenite gradually increased from the boundary of kamacite toward 2 μm interior and Fe profiles indicated an inverse pattern. There was no chemical difference between Neumann bands and the surrounding host kamacite. Quantitative chemical composition of representative points on their lines were measured, as listed in Table 2 together with the data reported by Rojkovič *et al.* (1995).

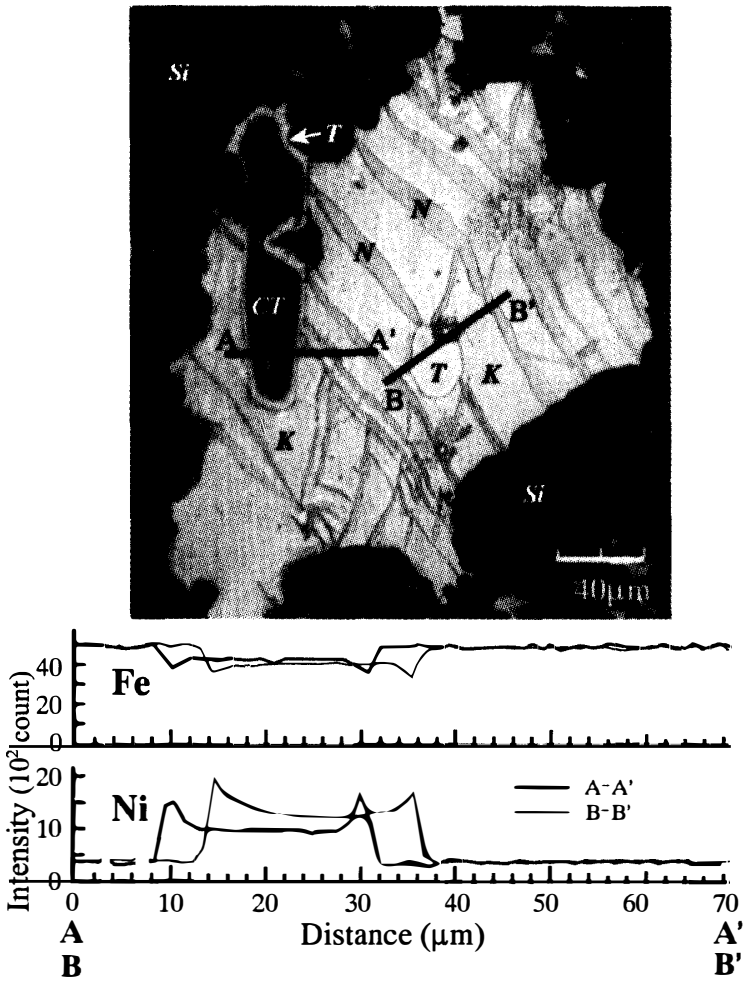

Fig. 7. A typical FeNi grain and analyzed lines of A–A′ and B–B′ by EPMA. K: kamacite, T: taenite, CT: cloudy zone, N: Neumann bands, Si: silicate.

When magnetic fluid was painted (Bitter Pattern) on the surface of other FeNi grains, the dense fluid accumulated on the full area of cloudy taenite, while no accumulation was formed on the periphery of cloudy taenite. The weak accumulation of the fluid was observed on taenite grains of 2–5 μm in size in plessite, while any visible accumulation was not seen on taenite grains. On some kamacite grains, the systematic zigzag weak-colored domain pattern appeared in the fluid with the interval of 2–6 μm. This may be the artificial mazy domain pattern created by mechanical polishing of the sample. In case of a etched FeNi grain in Fig. 8 (1), a kamacite grain (K) was sandwiched by cloudy taenite grains (a) and (b). The feature shows vague cloudy and clear zones in the grain (a), while typical cloudy taenite appeared on the grain (b). The Bitter pattern (2) shows both grains (a) and (b) are magnetic, but their peripheries are nonmagnetic. The sample B2t after thermal demagnetization to 630°C was acquired to IRM at 100 mT, and then it was polished to the Bitter pattern analysis. The result showed that the magnetic field accumulated on the cloudy taenite grains as observed in Fig. 8.

Table 2. Chemical compositions of FeNi grains in Rumanová measured by this study and Rojkovič et al. (1995).

1. This study

	1	2	4	5	6	8	9	3	7
Fe	94.412	95.256	92.087	93.093	94.065	93.253	93.628	78.736	75.738
Ni	6.45	6.925	5.879	6.759	6.546	6.269	6.972	17.664	25.52
Co	0.321	0.437	0.469	0.383	0.426	0.381	0.325	0.179	0.262
S	0.032	0.021	0.000	0.000	0.027	0.000	0.003	0.015	0.013
P	0.032	0.015	0.000	0.000	0.012	0.053	0.000	0.000	0.000
Total	101.25	102.654	98.435	100.235	101.076	99.956	100.928	96.594	101.533
	kamacite (wt%)							taenite (wt%)	

2. by Rojkovič *et al.* (1995)

	kamacite (wt%)							
	1	2	3	4	5	6	7	8
Fe	92.75	93.23	93.67	92.23	92.17	92.36	93.42	93.01
Ni	7.25	6.42	6.94	7.01	6.86	6.65	6.72	6.64
Total	100.00	99.65	100.61	99.24	99.06	99.01	100.14	99.65
	taenite (wt%)							
	1	2	3	4	5	6	7	8
Fe	66.84	81.97	61.80	60.69	61.49	81.93	79.60	68.71
Ni	32.77	17.80	37.51	38.61	38.76	18.16	19.84	30.45
Total	99.61	99.77	99.31	99.30	100.25	100.09	99.44	99.16

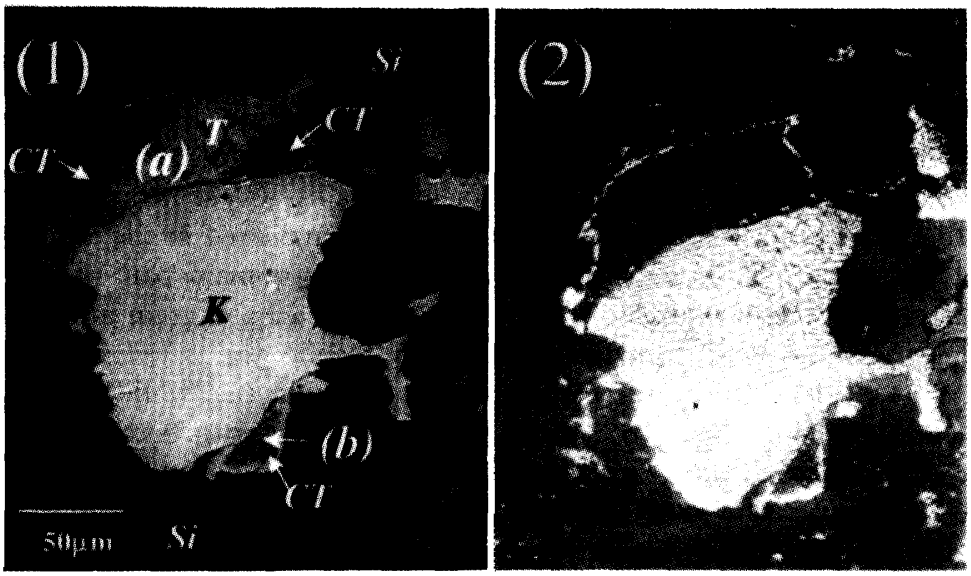

Fig. 8. A etched feature of FeNi grain (1) and its Bitter pattern feature (2). Grains (a) and (b) are cloudy taenite grains. K: kamacite, T: taenite, CT: cloudy zone, Si: silicate.

6. Discussions

The NRM directions of several ordinary chondrites were investigated using mutually oriented subsamples obtained from one block. Clustered NRM directions have been reported from Brewster (Weaving, 1962) and Wellman (Hamano and Matsui, 1983) but the surfaces of their samples were magnetically contaminated while falling through the atmosphere or on the earth's surface. Funaki *et al.* (1981) reported clustered NRM within a hemisphere from the matrix substances of an Antarctic chondrite, ALH-769. This sample has been protected from any artificial magnetic contaminations during the transportation from the sampling site in Antarctica to the laboratory. The original NRM direction of Rumanová is much more complicated; the samples A1–A5 are grouped as supported by $K=52$ and $\alpha_{95}=10.7$, while those of B1–B5 showed scattered NRM directions. These NRM distributions seem to resemble the characteristic, after if the soft (unstable) NRM component was removed by AF demagnetization to 30 mT.

The alteration of NRM for Rumanová due to terrestrial weathering characterized as W2 (Wlotzka, 1993) may be minor, because the dense accumulation of magnetic fluid is observed only on cloudy taenite and fine-grained taenite grains in plessite. If goethite and limonite resulting from weathering of kamacite, carry the dominant NRM, the fluid should accumulate on these minerals and a clearly defined discontinuity of thermal demagnetization curves (Fig. 3) should appear at 120°C related to the Curie point of these minerals. Unique unblocking temperature of NRM at 530°C is consistent with $T_C=530$°C and $TH_C=530$°C of the sample (Figs. 5 and 6), indicating that the NRM is carried by taenite with 48 wt%Ni but not by kamacite with 7 wt%Ni or other minerals.

From the evidence of Bitter pattern analysis, cloudy taenite is magnetic, while peripheral taenite is nonmagnetic, as shown in Fig. 8. Probably the Ni content of peripheral taenite is less than 30%, as analyzed the grain in Fig. 7, suggesting its parramagnetic behavior (above the Curie point of taenite at room temperature). It suggests that the shielding effect of the magnetic field irradiated from cloudy taenite can be ignored. The effect may act efficiently to the ferromagnetic taenite grains in plessite to the contrary, because kamacite surrounds them.

When Rumanová fell to the earth, its surface should acquire thermal remanent magnetization referred to the earth's magnetic field during cooling after atmospheric heating. However, the remagnetized layer is only 0.3–0.8 mm thick as estimated from the evidence of NRM variations of 5 Antarctic achondrites (Nagata, 1979). As the original surface of Rumanová seems to be removed more than several mm inward due to the weathering, the fusion crust and the remagnetized layer might be removed completely when the sample was found. So we concluded that the NRM of Rumanová was not affected by atmospheric heating.

NRM acquired by artificial magnetic contaminations such as a hand magnet etc. should align almost parallel in the small area, and the intensity must be stronger than the original one. The scattered NRMs directions of samples B1–B5 cannot be

explained by such contaminations, but the clustered ones of samples A1–A5 have a possibility of remagnetizing by such contamination. Their intensities, however, were not so different from each other as a range of $R=2.021$ to 5.717×10^{-2}Am^2/kg for samples A1–A5 and $R=0.432$ to 4.323×10^{-2} Am^2/kg for samples B1–B5. The AF demagnetization curves in Fig. 1 indicated similar NRM characteristics between the groups A and B. Consequently the NRM's in both groups may not be significantly different, and the strong artificial magnetic contaminations were not acquired taking the NRM intensities into consideration. Wasilewski and Dickinson (1998) pointed out if the ratio of NRM/SIRM (REM value) of a sample is larger than 0.01, the samples suffer artificial magnetic contaminations. The NRM intensities (5.755×10^{-2} Am^2/kg) and SIRM (7.921×10^{-1} Am^2/kg) of sample B1 of Rumanová give REM=0.07, suggesting only weak magnetic contaminations. Even if weak magnetic contamination was overprinted on the original NRM, it should be demagnetized by relatively weak AF demagnetization and thermal demagnetization as well as viscus remanent magnetization (VRM) etc., because it affects the multidomain (MD) grains. Consequently the reliable NRM can be taken by the demagnetization from 25 to 50 mT and from 330 and 530°C.

The IRM of Rumanová was not acquired in the applied magnetic field direction, but the IRM direction gradually shifted toward the field direction by the AF demagnetization up to 50 mT. It suggests there is strong magnetic anisotropy in larger FeNi grains characterized by MD but almost isotropy in the small ones of single domain size (SD). The observed large AMS supports this result, because the AMS is reflected predominantly by MD grains rather than SD ones. The strong anisotropy may be derived from the few larger MD grains with strong shape magnetic anisotropy in the sample. The random distribution of AMS axes may be given that MD grains in Rumanová have not been replaced by drastic mechanical deformation after solidification of magnetic grains with matrix substances. If Rumanová was compressed or extended by uniaxial kinematics, the directions of K_{min} or K_{max} of AMS of individual samples should point almost the same direction. The NRM and SIRM were decomposed into soft and hard components by AF demagnetization to 25 mT (Fig. 1 and Fig. 4). The ratio of hard NRM component is estimated to be about 20% in these demagnetization curves. Comparable hard NRM component of about 30% can be obtained by the thermal demagnetization between 330 and 530°C (Fig. 3). Namely, a large amount of NRM of Rumanová is insignificant paleomagnetically due to the magnetic soft and large anisotropy, while the part of the NRM obtained by AF demagnetization at more than 25 mT or by thermal demagnetization between 330 and 530°C is reliable.

The magnetic hump in the I_S-T curve seems to be explained due to newly formed magnetic minerals during heating between 80 and 150°C. One of the possibilities is formation of α-hematite (α-Fe_2O_3) by dehydration from goethite (α-FeOOH) which was described by Rojkovič *et al.* (1995), but its contribution may be rejected by following 3 reasons; (1) the saturation magnetization of α-hematite is less than 0.2% of that of iron suggesting under the detection in the I_S-T curve. (2) the Curie point of goethite at 120°C does not appear in the I_S-T

curve. (3) the dehydration of goethite should occur in the range 250–400°C, not occur in the range 80–150°C. The other plausible explanation of the hump is due to the formation of γ-hematite (γ-Fe_2O_3) and/or magnetite (Fe_3O_4) from lepidocrocite (γ-FeOOH) by the dehydration and/or reduction. In case of this estimation, however, estimated large magnetic hump should occur after its dehydration at 250–400°C. From these viewpoints, we could not specify the minerals resulting from the hump in present. As the formation of magnetite (T_C=580°C) from hydro iron oxide by reduction is rejected, the magnetic mineral related to T_C=550°C is inferred to be taenite with 48 wt%Ni. From the phase transition at T_C=580 and 700°C, Ni content of kamacite is inferred to be 7 wt%Ni.

From the results of microscopic observations and thermomagnetic analysis, magnetic minerals in Rumanová are considered to be mainly kamacite and taenite associated with small amounts of cloudy taenite, plessite, goethite and limonite. Goethite are weathering products on the earth as discussed by Rojkovič *et al.* (1995, 1997). Tetrataenite is the most important mineral as the stable NRM carrier of chondrites due to its high magnetic coercivity, but the coercivity of Rumanová, H_C =10.18 and H_{RC}=21.31 mT, is small compared with that of tetrataenite; if tetrataenite is present, the values must be larger than several 100 mT and decrease abruptly to several 10 mT by heating to higher than 550°C (Wasilewski, 1988). On the contrary, the coercivity values of Rumanová increased to H_C=16.04 and H_{RC}= 33.52 mT by heating to 850°C. Tetrataenite can be identified by the Bitter pattern configuration (Funaki *et al.*, 1986) due to the large magnetic gradient relative to its strong magnetization. The pattern indicated no accumulation of magnetic fluid along the peripheries of taenite and cloudy taenite where tetrataenite is usually formed in these regions (*i.e.*, Clark and Scott , 1980; Holland-Duffield *et al.*, 1991). From these viewpoints we concluded that tetrataenite is absent in Rumanová due to its disorder by heating more than 550°C. As tetrataenite grains in cloudy taenite are in the range of 15–650 nm in diameter and are surrounded by low Ni taenite (Reuter *et al.*, 1988), these disordered taenite grains are dominantly of SD size. This is the reason why Rumanová carries stable NRM.

Typical the Ni profile across a taenite grain in the non-shocked or weakly shocked chondrites shows the prominent M-shape pattern. The obscure M-shape pattern of Ni and inversed Fe pattern of Rumanová (Fig. 7) are considered due to the result of Ni diffusion at the periphery of the taenite by heating, as discussed by Bennett and McSween (1996). The maximum Ni content of taenite in Rumanová is 25.52 wt% in cloudy taenite in this study (Table 1) and 38.76 wt% by Rojkovič *et al.* (1995). These values are not sufficient for forming tetrataenite, because the Ni content in tetrataenite is 48–57 wt% (Clark and Scott, 1980). If the heating was higher than 550°C, the disorder of tetrataenite and the obscure M-shape pattern are explained simultaneously. Probably high-Ni and low-Ni grains in those cloudy taenite grains measured by EPMA were homogenized by such high temperature. Consequently medium Ni content was detected by above EPMA analyses. However, the high-Ni (52.2 at%) and a normal M-shape Ni profile of taenite have been reported in Rumanová by Rojkovič *et al.* (1997). A small amount of taenite with

48 wt%Ni certainly exists in Rumanová from the evidence of $T_C = 550°C$. This implies that Ni in a part of the high-Ni taenite does not diffuse completely toward the low-Ni taenite due to heterogeneous insufficient heating. Consequently the $T_C = 550°C$ and high-Ni taenite may be observed. The vague clear and cloudy zones in the magnetic grain (a) in Fig. 8 might be yielded by such insufficient diffusion.

No evidence of tetrataenite in cloudy taenite seems to be inferred from the H_C value. Tetrataenite was disordered by both of severe heating and pressure, although its disordering criterion by shock has not been demonstrated. Formation of plessite suggests the maximum temperature reached to about 525°C by shock S5 and S6 in most case (Bennett and McSween, 1996). Such high temperature is convenient for understanding the obscure M-shape pattern of Ni profiles. The upper limited temperature is defined to be less than 950°C, the melting temperature of FeS, from the evidence of the no polyclistallin-FeS grains. On the contrary, lower temperature is estimated. Since the existence of twinning of FeS keeping contact with some larger FeNi grains gives the shock pressure range of 10–20 GPa (Schmitt *et al.*, 1993). The peak pressure and temperature of silicate is estimated to be 5–20 GPa and 30–150°C from the shock metamorphism S3 (Stöffler *et al.*, 1991). Namely, very heterogenous temperature distributions are characterized in Rumanová. This distribution is a common features in the shocked chondrite, as discussed by Bennett and McSween (1996). From these viewpoints, the upper limit temperatures in Rumanová is defined to be 150°C for silicate and between 520 and 950°C for FeNi grains. Probably, when the parent body of Rumanová collided with the asteroids, the shock metamorphisms occurred.

When the shock pressure exceeds 13 GPa, the ferromagnetic magnetic αFe is transferred to antiferromagnetic (nonmagnetic) εFe, subsequently the transformation from εFe to αFe should occur after the shock wave passed through the sample, assuming remagnetization was due to the ambient magnetic field. The pressure of phase transition decreases depending on the Ni content in FeNi, as about 10 GPa for 80%Fe 20%Ni (see Wasilewski, 1976). It may be, therefore, that the NRM carrier consisting of kamacite in Rumanová were demagnetized and subsequently remagnetized lower shock pressure. Neumann bands are shock-produced mechanical twinning lamellae which form along the (211) plains of the kamacite (Wasson, 1974). Deformed spindle Neumann bands, therefore, indicate deformation of the single crystals grains. The deformation, however, is not affected to the fabric of the magnetic grains in Rumanová, because of the random distribution of magnetic anisotropy axes (K_{max} and K_{min}) among the samples.

A plausible acquisition mechanism of the clustered and scattered NRM's of Rumanová may be interpreted as follows. (1) Rumanová was metamorphosed at 700°C characterized by the classification H5. Tetrataenite might be formed and be magnetized in the ambient magnetic field direction during the cooling stage, if the magnetic field was there in the parent body. (2) At collision with asteroids, the majority tetrataenite grains were disordered due to shock heating between 550°C and 950°C, furthermore, the phase transition to nonmagnetic, εFe phase by shock demagnetized FeNi grains. The temperature of the FeS and silicate grains in the

matrix did not increase more than 150°C at that time. (3) Rumanová was cooled down extremely weak magnetic field in the parent body after passing through the shock waves. Probably, the local magnetic fields were influenced to the magnetization of the small samples: these samples include a few larger FeNi grains up to 1mm (Rojkovič *et al.*, 1997), whose grains should have spontaneous magnetization due to their shape and crystalline magnetic anisotropies. This may be the reason why the individual samples have NRM. If extremely strongly magnetized FeNi grains are there in the sample, a part area surrounding the grain was magnetized toward almost the same NRM direction, as observed in samples A1–A5. On the contrary, if the grains do not have such strong magnetization, the NRM direction should be widely scattered among the small samples, as observed in samples B1–B5. The SD taenite grains in cloudy taenite and fine-grained taenite grains in plessite carry the NRM in the cooling stage lower than 530°C. We conclude, therefore, that the stable NRM of Rumanová is not the original but it was remagnetized during cooling after shock metamorphism.

6. Results

Rumanová carries NRM stable against AF demagnetization to more than 50 mT and the directions are variable depending on the samples. The significant NRM is carried by the SD size of taenite grains with 48 wt%Ni in cloudy taenite, while the contribution of kamacite with 7 wt%Ni to NRM is negligibly small. It seems not to be drastically disturbed by artificial or natural magnetic contaminations on the earth. Insignificant NRM component carried by the MD size grains has the large magnetic anisotropy with random orientations, but it is demagnetized by AF demagnetization more than 25 mT and thermal demagnetization between 330 and 530°C.

The shock metamorphisms of Rumanová were described from the opaque minerals based on the following evidence; obscure M-shape pattern of the Ni profiles in taenite, lack of tetrataenite, twinning of FeS grains and deformation of FeNi grains. Tetrataenite was disordered to taenite by shock heating to between 525°C and 950°C, but the matrix substances were not heated to more than 150°C. Probably present NRM in Rumanová was acquired during the cooling stage from 530°C after shock metamorphism in the local magnetic field due to cloudy taenite and plessite grains with strong spontaneous magnetization due to the shape and crystalline magnetic anisotropies.

Acknowledgments

The authors wish to thank Drs. I. Imae and M. Ozima, National Institute of Polar Research, for the measurement of chemical composition of FeNi grains by EPMA and for helpful discussions.

References

Bennett, M. E. and McSween, H. Y., Jr. (1996): Shock features in iron-nickel metal and troilite of L-group ordinary chondrites. Meteorit. Planet. Sci., **31**, 255–264.

Clark, R. S., Jr. and Scott, E. R. D. (1980): Tetrataenite-ordered FeNi, a new mineral in meteorites. Am. Mineral., **65**, 624–630.

Funaki, M., Túnyi, I., Orlický, O. and Porubčan, V. (1999): A preliminary study of the basic magnetic properties of Rumanová (H5) chondrite found in Slovakia. Contrib. Geophys. Geodesy, **29** (3), 1–8.

Funaki, M., Nagata, T. and Momose, K. (1981): Natural remanent magnetization of chondrules, metallic grains and matrix of an Antarctic chondrite, ALH-769. Mem. Natl Inst. Polar Res., Spec. Issue, **20**, 300–315.

Funaki, M., Nagata, T. and Danon, J. A. (1986): Magnetic properties of lamellar tetrataenite in Toluca iron meteorite. Mem. Natl Inst. Polar Res., Spec. Issue, **41**, 382–393.

Hamano, Y. and Matsui, M. (1983): Natural remanent magnetization of the Wellman meteorite. Geophys. Res. Lett., **10**, 861–864.

Holland-Duffield, C. E., Williams, D. B. and Goldstein, J. I. (1991): The structure and composition of metal particles in two type 6 ordinary chondrites. Meteoritics, **26**, 97–103.

Nagata, T. (1979): Natural remanent magnetization of the fusion crust of meteorites. Mem. Natl Inst. Polar Res., Spec. Issue, **15**, 253–272.

Reuter, K. B., Williams, D. B. and Goldstein, J. I. (1988): Low temperature phase transformations in the metallic phases of iron and stony-iron meteorites. Geochim. Cosmochim. Acta, **52**, 617–626.

Rojkovič, I., Porubcan, V. and Siman, P. (1995): Nalez meteoritu pri obci Rumanová. Mineralia Slovaca, **27**, 331–342.

Rojkovič, I., Siman, P. and Porubcan, V. (1997): Rumanová H5 chondrite, Slovakia. Meteorit. Planet. Sci., **32**, A151–A153.

Schmitt, R. T., Deutsch, A. and Stöffler, D. (1993): Shock effects in experimentally shocked samples of the H6 chondrite Kernouvè (abstract). Meteoritics, **28**, 431–432.

Stöffler, D., Keil, K. and Scott, E. R. D. (1991): Shock metamorphism of ordinary chondrites. Geochim. Cosmochim. Acta, **55**, 3845–3867.

Wlotzka, F. (1993): A weathering scale for the ordinary chondrites (abstract). Meteoritics, **28**, 460.

Wasilewski, P. (1976): Shock-loading meteoritic b.c.c metal above the pressure transition: Remanent-magnetization stability and microstructure. Phys. Earth Planet. Int., **11**, 5–11.

Wasilewski, P. (1988): Magnetic characterization of the new magnetic mineral tetrataenite and its contrast with isochemical taenite. Phys. Earth Planet. Int., **52**, 150–158.

Wasilewski, P. and Dickinson, T. (1998): The role of magnetic contamination in meteorites. submitted to Meteorit. Planet. Sci.

Wasson, J. T. (1974): Meteorites. Springer-Verlag, 161 p.

Weaving, B. (1962): The magnetic properties of the Brewstger meteorite. Geophys. J., **7**, 203–211.

(Received September 6, 1999; Revised manuscript received December 27, 1999)